

Terahertz homodyne self-mixing transmission spectroscopy

Till Mohr,^{1,a)} Stefan Breuer,¹ Dominik Blömer,¹ Marcello Simonetta,^{2,b)} Sanketkumar Patel,¹ Malte Schlosser,¹ Anselm Deninger,³ Gerhard Birkl,¹ Guido Giuliani,⁴ and Wolfgang Elsässer^{1,c)}

¹Institute for Applied Physics, Technische Universität Darmstadt, Schlossgartenstr. 7, 64289 Darmstadt, Germany

²Dipartimento di Ingegneria Industriale e dell'Informazione, Università di Pavia, Via Ferrata 1, i-27100 Pavia, Italy

³Toptica Photonics AG, Lochhamer Schlag 19, 82166 Gräfelfing, Germany

⁴Dipartimento di Ingegneria Civile e Architettura, Università di Pavia, Via Ferrata 3, i-27100 Pavia, Italy

(Received 17 November 2014; accepted 2 February 2015; published online 12 February 2015)

A compact homodyne self-mixing terahertz spectroscopy concept is experimentally investigated and confirmed by calculations. This method provides amplitude and phase information of the terahertz radiation emitted by a photoconductive antenna in a transmission experiment where a rotating chopper wheel serves as a feedback mirror. As a proof-of-principle experiment the frequency-dependent refractive index of Teflon is measured. © 2015 AIP Publishing LLC.

[<http://dx.doi.org/10.1063/1.4908059>]

In recent years, terahertz technologies have gained great interest, due to their huge potential in fundamental research and industrial applications including nondestructive testing, biomedical diagnostics, security screening, and pollutant monitoring.^{1–3} A multitude of competing techniques for the generation and detection of terahertz radiation have been developed, ranging from electronic^{4,5} and optoelectronic^{6,7} to fully optical schemes.^{8–10} One of the most promising approaches involves optoelectronic terahertz generation with the help of photoconductive antennas (PCAs): Photoconductive switches allow for the generation of broadband terahertz pulses, with applications in time domain spectroscopy,¹¹ whereas so-called photomixers translate the beat signal of two lasers into continuous-wave (CW) terahertz radiation, with the perspective for high-resolution finger-print spectroscopy.^{12,13} Advantages of the latter technique include robustness, phase sensitivity, and a good signal-to-noise ratio, which makes it an ideal option for many scientific and industrial tasks.¹⁴ Promising progress towards improving the compactness of terahertz sources has been achieved by combining the terahertz source (transmitter) and detector (receiver) into one device as realized for example, by quantum cascade laser self-mixing.¹⁵ Very recently, a similar approach for the generation and detection of broadband terahertz pulses has been reported involving a setup that includes a femtosecond laser and a photoconductive switch.¹⁶

In this paper, we demonstrate a terahertz spectroscopy concept by combining both CW-terahertz radiation generation and phase-sensitive detection in one PCA, which results in a significantly reduced complexity and cost of the terahertz spectroscopy setup.

The compact experimental set-up is depicted schematically in Fig. 1. Two multiplexed tunable external-cavity diode lasers (ECDLs) emit at wavelengths around 794 nm. Both

ECDLs provide an optical output power of approximately 80 mW and possess a spectral line width smaller than 1 MHz. The two laser beams are coupled into one polarization-maintaining single-mode fiber (PMF). The resulting optical beat signal impinges on a fiber-coupled PCA (FC-PCA)(GaAs-based photomixer, model EK-000831, TOPTICA Photonics). The FC-PCA features an interdigitated finger structure and a logarithmic spiral antenna with three turns, which emits the terahertz radiation at the difference frequency of the two lasers. A hyperhemispherical silicon lens (SiL) focuses the terahertz beam approximately 40 mm behind the PCA, with a beam waist w_0 of around 2.5 mm (for 0.3 THz). The PCA is electrically connected to a 9 V battery that provides a constant bias voltage. A revolving chopper wheel (RCW)(Scitec Instruments Inc.) mounted on a linear translation stage (ESP300, Newport Inc.) is placed within the Rayleigh length of the terahertz radiation, which we estimate to about 20 mm for a terahertz-wave frequency of 0.3 THz. Its surface generates a back-reflection that is modulated at a chopping frequency up to 2.6 kHz. The chosen chopper wheel

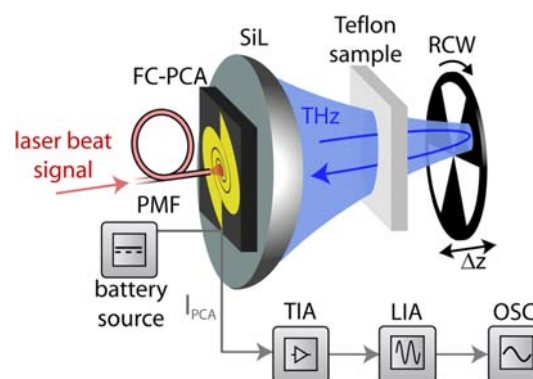


FIG. 1. Schematic of the experimental set-up. PMF, polarization-maintaining single-mode fiber; FC-PCA, fiber-coupled photoconductive antenna; SiL, silicon lens; RCW, revolving chopper wheel; TIA, transimpedance amplifier; LIA, lock-in amplifier, OSC—digital oscilloscope.

^{a)}Email: till.mohr@physik.tu-darmstadt.de

^{b)}Present address: Istituto Nazionale di Fisica Nucleare Sezione di Pavia, Via Bassi 6, i-27100 Pavia, Italy.

^{c)}Also at: Center of Smart Interfaces, Technische Universität Darmstadt, Alarich-Weiss-Straße 10, 64287 Darmstadt, Germany.

aperture allows to minimize diffraction limiting effects.¹⁷ Via the translation stage, the phase between the laser beat signal and the back-reflected terahertz radiation is varied. The back-reflection gives rise to an AC photocurrent in the FC-PCA. This current signal is electrically amplified by a transimpedance amplifier (TIA) (DLPCA-200, FEMTO), which separates AC and DC current contributions and amplifies the alternating current by a factor of 10^5 V/A. The output signal of the TIA and the electrical reference frequency of the chopper wheel are fed to a lock-in amplifier (LIA) and the resulting amplitude and phase signals are monitored on a digital two-channel oscilloscope (Tektronix TDS3022). A phase-dependent homodyne self-mixing (HSM) signal, which is proportional to the electric field of the back-reflected terahertz wave, is obtained by a multiplication of the measured amplitude and the cosine of the phase. The two lasers emit at wavelengths of 795.93 nm and 797.07 nm, corresponding to a frequency (wavelength) of the generated terahertz radiation of 0.539 THz ($556 \mu\text{m}$). The experimentally obtained HSM signal is depicted in Fig. 2 as a function of the spatial displacement of the RCW, which is translated over 1.2 mm with a constant velocity of $40 \mu\text{m/s}$. A sinusoidal signal with a periodicity of half of the terahertz wavelength is evident, since the optical delay of the terahertz wave corresponds to twice the RCW displacement. Fitting a sine function to the data yields a period of $275 \mu\text{m}$, which is in good agreement with the value of $278 \mu\text{m}$ as expected from the wavelengths of the two lasers. The detected HSM signal originates from interference generated by a nonlinear product of the back-reflected terahertz wave and the time-dependent conductance of the PCA.

In the following, we model this effect and calculate the time-dependent total current $I(t)$ in the PCA as the product of the induced terahertz voltage $V(t)$ and electrical conductance $G(t)$. The time-varying conductance $G(t)$ is modulated at the beat frequency of the two lasers

$$G(t) = G_{\text{Dark}} + G_{\text{THz}} \times (1 + \sin(\omega t)), \quad (1)$$

where G_{Dark} is the conductance without any laser radiation impinging on the PCA, ω is the frequency of the beat signal, and G_{THz} is the conductance proportional to the total average laser power. Besides the constant voltage bias V_0 applied to the PCA, we consider a time- and terahertz phase-dependent voltage $V_{\text{FB}}(t)$, induced by the back-reflected terahertz radiation. Considering the voltage $V_{\text{FB}}(t)$ with its proportionality

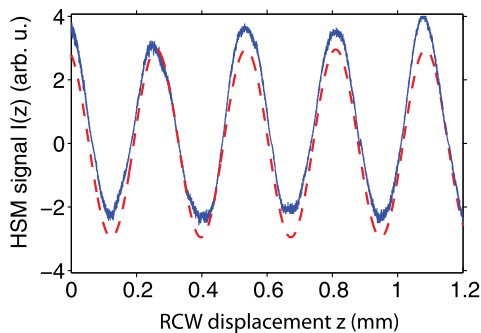


FIG. 2. (Solid, blue) Measured HSM signal versus displacement z of the reflecting RCW. (Dashed, red) Curve fitting of the measured data by a sine function.

factor V_{FB0} , we obtain the following expression for the total current:

$$\begin{aligned} I(t, \phi) &= G(t) \times V(t) = G(t) \times (V_0 + V_{\text{FB0}} \sin(\omega t + \phi)) \\ &= G_{\text{Dark}} V_0 + G_{\text{THz}} V_0 + G_{\text{THz}} V_0 \sin(\omega t) \\ &\quad - \frac{V_{\text{FB0}} G_{\text{THz}}}{2} \cos(2\omega t + \phi) + G_0 V_{\text{FB0}} \sin(\omega t + \phi) \\ &\quad + \frac{V_{\text{FB0}} G_{\text{THz}}}{2} \cos(\phi). \end{aligned} \quad (2)$$

The mean value of this current on time scales much longer than the period of the terahertz wave is then given by

$$\langle I(t, \phi) \rangle_{t \gg T_{\text{THz}}} = G_{\text{Dark}} V_0 + G_{\text{THz}} V_0 + \frac{V_{\text{FB}} G_{\text{THz}}}{2} \cos(\phi). \quad (3)$$

The last term in Eq. (3) provides information on the path length travelled by the terahertz wave to the RCW and back, since $\phi = 2ks$, where k is the wave number of the terahertz field and s is the displacement of the RCW. The upper part of Fig. 3 depicts the total instantaneous PCA current in the time-domain for a back-reflected wave of 0.539 THz, calculated from Eq. (2) with typical values of $0.04 \mu\text{S}$, $1 \mu\text{S}$, and 1mV for G_{Dark} , G_{THz} , and V_{FB} , respectively, and omitting the DC contribution of V_0 . Here, the total current clearly exhibits a non-vanishing mean value on time scales much longer than the terahertz period, caused by the nonlinear product in Eq. (2). Furthermore, with increasing displacements, a decreasing mean current is found, which is indicated by a decreasing minimum towards higher displacements depicted in the top of Fig. 3. The calculated mean current within the PCA over a displacement from 0 to 1.2 mm and for a back-reflected wave with frequency of 0.539 THz exhibits a sinusoidal shape with a period of $\lambda/2$, which is depicted in the bottom part of Fig. 3.

In order to exploit the phase-sensitivity of the presented HSM method and thus to validate the proposed method, we will now describe a measurement of the refractive index of Teflon. Teflon samples of different thickness are placed between the PCA and the RCW as indicated in Fig. 1. The laser wavelengths are tuned to 797.08 nm and 797.44 nm

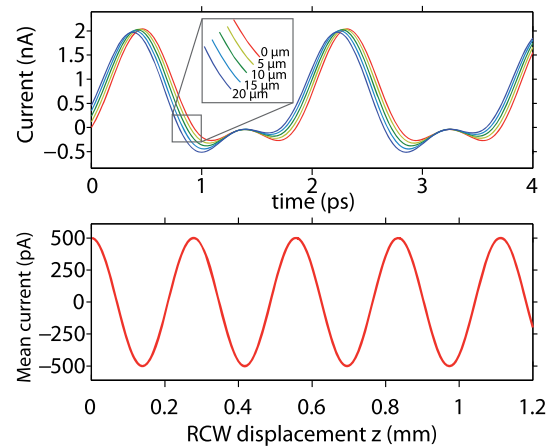


FIG. 3. Simulations of the photocurrent induced in the PCA by a back-reflected 0.539 THz wave. (Top) Calculated PCA current for a RCW displacement of 0, 5, 10, 15, and $20 \mu\text{m}$, neglecting the contribution of the constant bias voltage V_0 . (Bottom) Calculated mean PCA current versus RCW displacement, on time scales much longer than the terahertz period.

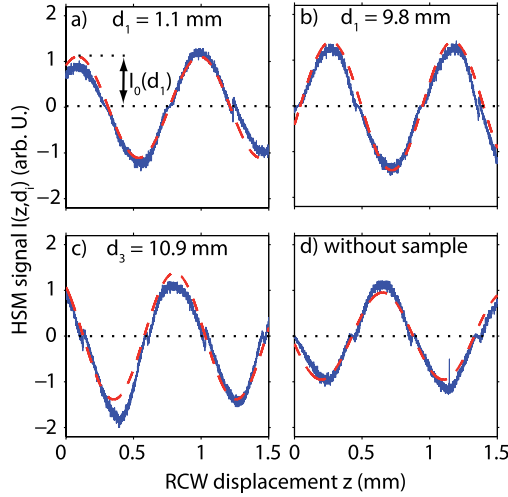


FIG. 4. Measured HSM signals as a function of the displacement (z) of the RCW for selected Teflon samples of thickness $d_1 = 1.1$ mm (a), $d_2 = 9.8$ mm (b), $d_3 = 10.9$ mm (c), and without Teflon sample (d) (solid). Fit curves according to Eq. (4) (dashed).

resulting in a terahertz frequency of 0.17 THz, thus, a periodicity of the HSM signal of $898 \mu\text{m}$ is expected. For each sample, the HSM signal is recorded over a total linear translation of the RCW of 1.6 mm, with each scan starting from the same position. The experimental results are plotted in Fig. 4 for selected Teflon samples of thickness $d_1 = 1.1$ mm (a), $d_2 = 9.8$ mm (b), $d_3 = 10.85$ mm (c) and for a reference measurement without Teflon sample (d). All of the traces show the expected sinusoidal shape of the HSM signal with a periodicity of $900.5 \mu\text{m}$. The phase of the HSM signals varies with the sample thickness which can be explained by the different optical path lengths of the terahertz wave within the sample. In fact, the total terahertz path consists of 3 contributions: the base displacement of the RCW (s_0), the path travelled through the linear translation stage (z), and the additional optical path length by the Teflon sample ($d \times (n - 1)$).

To retrieve the refractive index of Teflon at 0.17 THz, we fit the following set of equations to the data:

$$I(z, d_i) = I_0(d_i) \times \cos\left(\frac{4\pi}{\lambda} [s_0 + z + (d_i + \Delta d(d_i)) \times (n_{\text{Teflon}} - 1)]\right). \quad (4)$$

Here, I_0 denotes the amplitude of the HSM signal, λ the terahertz wavelength, d the geometric thickness of the Teflon sample measured with a caliper, Δd a correction factor considering a possible uncertainty of this thickness measurement and n_{Teflon} the real part of the refractive index of Teflon. The result of the curve fitting is plotted in Fig. 4 together with the experimental data. A good qualitative agreement between modeling results and experiment is obtained for the individual Teflon samples. A summary of the evaluated parameters is given in Table I. The curve fitting yields a terahertz wavelength of $1807 \mu\text{m}$. Although the obtained value of

TABLE I. Curve fitting parameters used for the determination of the refractive index of Teflon. i denotes the Teflon sample index, where $i = (1, 2, 3)$ corresponds to the sample thicknesses of (1.1, 9.8, 10.9) mm.

Parameter	Value
Amplitude of HSM signal: I_0 (no Teflon)	0.95
$I_0(d_i)$	1.11, 1.41, 1.39
Thickness correction $\Delta d(d_i)$	(291, 42, -103) μm
for teflon sample	
Start displacement of RCW s_0	40 mm
Wavelength of terahertz radiation λ	1807 μm
Refractive index of Teflon n_{Teflon}	1.41

Δd_i is surprisingly high, which could be attributed to possible deviations of the ideally plane sample surface or deposits on the surface, the value of the achieved terahertz wavelength agrees within 0.6% with the calculated wavelength of $1796 \mu\text{m}$, which is derived from measurements of the optical spectra of the two lasers. Furthermore, the measured refractive index of Teflon amounts to 1.41 at 0.17 THz, which is very close to the literature value of 1.44.¹⁸

In conclusion, we have demonstrated an experimental method for the generation and detection of CW-terahertz radiation utilizing only one PCA. The PCA simultaneously acts as transmitter and receiver for continuous-wave terahertz radiation which is reflected off a rotating chopper wheel. We have determined the refractive index of Teflon. This terahertz spectroscopic setup infers a cost reduction and relaxes the demand on high laser power as only one PCA is needed. The proposed method lends itself to the realization of compact terahertz assemblies and may find industrial usage e.g., for measurements of the thickness or refractive index of polymer components.

We acknowledge support from Sensors Towards Terahertz within the LOEWE platform (1502-2995-11). S. Breuer acknowledges support through the Adolf Messer Foundation.

¹W. Zouaghi, M. D. Thomson, K. Rabia, R. Hahn, V. Blank, and H. G. Roskos, *Eur. J. Phys.* **34**, S179 (2013).

²A. J. Seeds, M. J. Fice, Ka. Balakier, M. Natrella, O. Mitrofanov, M. Lamponi, M. Chtioui, F. van Dijk, M. Pepper, G. Aeppli, A. G. Davies, P. Dean, E. Linfield, and C. C. Renaud, *Opt. Express* **21**, 22988 (2013).

³H.-J. Song and T. Nagatsuma, *IEEE Trans. Terahertz Sci. Technol.* **1**, 256 (2011).

⁴M. Feiginov, C. Sydlo, O. Cojocari, and P. Meissner, *Appl. Phys. Lett.* **99**, 233506 (2011).

⁵A. Lisauskas, M. Bauer, S. Boppel, M. Mundt, B. Khamaisi, E. Socher, R. Venckevičius, L. Minkevičius, I. Kašalynas, D. Seliuta, G. Valušis, V. Krozer, and H. G. Roskos, *J. Infrared Millim. Terahertz Waves* **35**, 63 (2014).

⁶E. R. Brown, K. A. McIntosh, F. W. Smith, M. J. Manfra, and C. L. Dennis, *Appl. Phys. Lett.* **62**, 1206 (1993).

⁷K. A. McIntosh, E. R. Brown, K. B. Nichols, O. B. McMahan, and W. F. DiNatale, *Appl. Phys. Lett.* **67**, 3844 (1995).

⁸Q. Y. Lu, Q. Y. N. Bandyopadhyay, S. Slivken, Y. Bai, and M. Razeghi, *Appl. Phys. Lett.* **104**, 221105 (2014).

⁹B. S. Williams, *Nat. Photonics* **1**, 517 (2007).

¹⁰R. Köhler, A. Tredicucci, F. Beltram, H. E. Beere, E. H. Linfield, A. G. Davies, D. A. Ritchie, R. C. Iotti, and F. Rossi, *Nature* **417**, 156 (2002).

- ¹¹N. Vieweg, F. Rettich, A. Deninger, H. Roehle, R. Dietz, T. Göbel, and M. Schell, *J. Infrared Millim. Terahertz Waves* **35**, 823 (2014).
- ¹²S. Preu, G. Döhler, S. Malzer, L. Wang, and A. Gossard, *J. Appl. Phys.* **109**, 061301 (2011).
- ¹³S. Preußler, N. Wenzel, R. Braun, N. Owschmikow, C. Vogel, A. Deninger, A. Zadok, U. Woggon, and T. Schneider, *Opt. Express* **21**, 23950 (2013).
- ¹⁴D. Saeedkia, *Handbook of Terahertz Technology for Imaging, Sensing and Communications* (Elsevier Science & Technology, 2013).
- ¹⁵P. Dean, Y. L. Lim, A. Valavanis, R. Kliese, M. Nikolić, S. P. Khanna, M. Lachab, D. Indjin, Z. Ikonić, P. Harrison, A. D. Rakić, E. H. Linfield, and A. G. Davies, *Opt. Lett.* **36**, 2587 (2011).
- ¹⁶S. Busch, T. Probst, M. Schwerdtfeger, R. Dietz, J. Palací, and M. Koch, *Opt. Express* **22**, 16841 (2014).
- ¹⁷D. M. Mittleman, R. H. Jacobsen, and M. C. Nuss, *IEEE J. Sel. Top. Quantum Electron.* **2**, 679–692 (1996).
- ¹⁸P. Cunningham, N. Valdes, F. Vallejo, L. Hayden, B. Polishak, X. Zhou, J. Luo, A. Jen, J. Williams, and R. Twieg, *J. Appl. Phys.* **109**, 043505 (2011).